Indian Journal of Pure & Applied Physics
Vol. 59, May 2021, pp. 365-371

Effect of Tilted Electric Field and Magnetic Field on the Energy Levels, Binding Energies and Heat Capacity of Donor Impurity in GaAs Quantum Dot

Amal Abu Alia, Ayham Shaer, Mahmoud Ali & Mohammad K. Elsaid*

Department of Physics, Faculty of Science, An- Najah National University, Palestine Nablus, P400

Received 5 January 2020; accepted 5 February 2021

The Hamiltonian of an electron confined in a parabolic quantum dot in the presence of perpendicular magnetic field, donor impurity, and tilted electric field, has been solved by employing an exact diagonalization method. All the energy matrix elements have been derived in analytical forms. We have displayed the variation of the computed energy levels, binding energy and heat capacity of the quantum dot with the physical Hamiltonian parameters like: external magnetic and electric fields, confining strength, tilt angle and temperature. It's found that the binding energy increases as the magnetic field increases. However, it decreases as the electric field increases. The dependence of the heat capacity on the electric field and magnetic fields and impurity has also been investigated. The calculated results show that heat capacity increases as the electric field increases, while it decreases with the enhancement of the magnetic field. In addition, the presence of the donor impurity is found to enhance the heat capacity. The present results are consistent with those reported in the literature.

Keywords: Heat capacity, Quantum Dot, Binding energy

1 Introduction

Technological advancement necessitates smaller and faster machines. As a result, nanoscience has become a fertile ground for researchers[1-9], to investigate the properties of low-dimensional hetero structures. Among these structures, quantum dots (QDs) have attracted the attention of many researchers[10-12] due to their tunable properties and ability to be fabricated in a variety of shapes and sizes[7-9]. Several experimental and theoretical studies have been made out to explore the effects of applied magnetic and electric fields, pressure, temperature, impurity, and Rashba interaction on the electronic and thermomagnetic properties of QDs.[6-44]

The study of hydrogenic impurity in the low dimensional structure has a great influence on the electron's mobility, electronic, magnetic and optical properties[4]. Rezaei *et al.*[37] had studied the effects of external fields on the spectral properties of the donor impurity by direct numerical integration method, where the energy matrix elements had been performed numerically. In this work, we will implement the Exact Diagonalization Method (EDM) to investigate the system of the donor impurity in a QD in the presence of external fields and then use the computed spectra to calculate the thermal quantities like heat capacity($\boldsymbol{C_v}$). All the matrix elements in the QD Hamiltonian are produced and given in a closed analytic form which greatly simplified the process of computing the numerical results.

We consider a QD which is made from Gallium Arsenide (GaAs) encircled by a semiconductor hetero structure made of Aluminum Gallium Arsenide (AlGaAs)[37] with a parabolic confinement potential. We consider a confined electron in the XY- plane with a uniform magnetic field B applied along Z direction, and a tilted electric field (F) with angles θ and ϕ as illustrated in Fig. 1with the presence of lateral parabolic confinement potential and hydrogenic impurity.

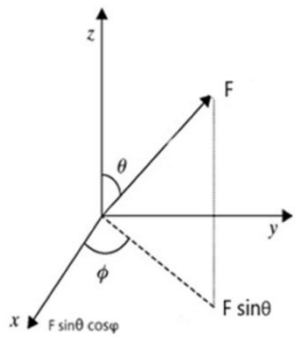

Fig. 1 — Demonestration of the tilted electric field.

*Corresponding author (E-mail: mkelsaid@najah.edu)

2 Theory

The required steps which lead to computation of the desired QD spectra are discussed in this section which are: (i) QD Hamiltonian of donor impurity in presence of external fields (ii) calculation of the energy matrix expressions, (iii) statistical average energy and (iv) heat capacity.

The Hamiltonian of a QD in two-dimensions (2D), is given by:

$$\hat{H} = \frac{p^2}{2m^*} + V_c(r) \quad \text{... (1)}$$

m^* and $\vec{P}$ is the electron's effective mass and its kinetic momentum, respectively, $V_c(r)$ is the confinement potential, in present work, the confinement takes the parabolic form with frequency ω_0 as:

$$V_c(r) = \frac{1}{2} m^* \omega_0^2 r^2 \quad \text{… (2)}$$

In this study, we looked at several physical parameters such as magnetic field, titled electric field, and impurity, all of which have a significant impact on the Hamiltonian of the system.

The vector potential $\vec{A}$ includes the effect of a magnetic field, as:

$$\vec{A} = \frac{\vec{B} \times \vec{r}}{2} \quad \text{… (3)}$$

Where, $\vec{r}$ denotes the electron's radial position, and $\vec{B}$ denotes for the magnetic field strength. The effect of the donor impurity arises in the Hamiltonian as a new attractive coulomb type term $(-\frac{e^2}{\epsilon r})$, where, e, ϵ is the electron's charge and the GaAs dielectric constant, respectively. We used effective Bohr radius a^*(effective Rydberg R^*) as a unit for length (energy) in our calculations.

The effect of electric field can be seen in the Hamiltonian as$e\boldsymbol{F}.\boldsymbol{r} = -eFrsin\theta cos\varphi$. Where, F is the electric field strength, θ and ϕ are angles illustrated in Fig. 1, ϕ and $r$are the polar coordinates, while the tunable parameter θdescribes the angle between $F$and the Z-direction.

The total Hamiltonian using the polar coordinate (r, ϕ) is given by[31,37]

$$\hat{H} = -\frac{1}{2m^*}\left(\vec{P} + \frac{e}{c}\vec{A}\right)^2 - \frac{e^2}{\epsilon r} + e\,\vec{F}\,.\vec{r} + \frac{1}{2} m^* \omega_0^2 r^2 \quad \text{… (4)}$$

Choosing the symmetric gauge for vector potential, $\vec{A} = B\,(-y, x, 0)$, the QD Hamiltonian can be written as[37]:

$$H = -\frac{\hbar^2}{2m^*}\nabla_r^2 + \frac{1}{2} m^* \omega_0^2 r^2 + \frac{1}{8} m^* \omega_c^2 r^2 - \frac{e^2}{\epsilon r} + eFr\,sin\theta\,cos\phi + \frac{1}{2}\,\hbar\omega_c L_z \quad \text{… (5)}$$

Where, $s(L_z)$ denotes the electron spin (z-component of angular momentum)

The total Hamiltonian given by Eq.5 can be separate for two Hamiltonians as:

$$H = H_0 + H_1 \quad \text{… (6)}$$

Where,

$$H_0 = -\frac{\hbar^2}{2m^*}\nabla_r^2 + \frac{1}{2} m^* r^2 \left(\frac{1}{2}\omega_c^2 + \omega_0^2\right) \quad \text{… (7)}$$

and,

$$H_1 = -\frac{e^2}{\epsilon r} + eFr\,sin\theta\,cos\phi + \left[\frac{1}{2}\,\hbar\omega_c\right] L_z \quad \text{… (8)}$$

Where, ω_c is magnetic field cyclotron frequency given by:

$$\omega_c = \frac{eB}{m^* c} \quad \text{… (9)}$$

H_0 is a Hamiltonian for harmonic oscillator with effective frequency ω_{eff}.

$$\omega_{eff}^2 = \frac{1}{4}\omega_c^2 + \omega_0^2 \quad \text{… (10)}$$

with well-known eigen energy E_{nm} and eigen function Ψ_{nm}, , given by Fock-Darwin states[38-39]:

$$\Psi_{nm}(r, \phi) = N_{nm}\,\frac{e^{im\phi}}{\sqrt{2\pi}}(\beta r)^{|m|} e^{-\frac{\beta^2 r^2}{2}} L_n^{|m|}(\beta^2 r^2) \quad \text{… (11)}$$

and,

$$E_{nm} = (2n + |m| + 1)\hbar\omega_{eff} \quad \text{… (12)}$$

$L_n^{|m|}$ referred to the Laguerre polynomial, $n$and m is the radial and magnetic quantum numbers, respectively, where the constant N_{nm} is obtained from normalization condition to be:

$$N_{nm} = \sqrt{\frac{2n!\,\beta^2}{(2n+|m|)!}} \quad \text{… (13)}$$

with

$$\beta = \left(\frac{m^2\,\omega_{eff}}{\hbar}\right)^{1/2} \quad \text{… (14)}$$

The fact that the presence of second part in Eq. 6, makes it impossible to achieve the analytical solution. As an effective technique, we use EDM to solve the QD system. In order to reach our goal, we aim to construct a Hamiltonian matrix as:

$$H_{nm,n'm'} = \langle \Psi_{nm} | \hat{H} | \Psi_{n'm'} \rangle \quad \ldots (15)$$

The QD eigen values are then computed by diagonalzing the matrix ($H_{nm,n'm'}$). An important step, in this work, was to produce the integrals of the energy matrix elements ($H_{nm,n'm'}$) in the simplest closed form in order to reduce the computational the amount of time required for the diagonalization process.

The Hamiltonian matrix elements are derived in the following form:

$$\langle \Psi_{nm} | H_0 | \Psi_{,n'm'} \rangle = (2n + |m| + 1)\omega_{eff}\, \delta_{nn'}\delta_{mm'} \quad \ldots (16)$$

$$\left\langle \Psi_{nm} \left| \frac{1}{2}\, \hbar\omega_c\, L_z \right| \Psi_{,n'm'} \right\rangle = \left(\frac{1}{2}\, m\, \omega_c\right) \delta_{nn'}\delta_{mm'} \quad \ldots (17)$$

$$\left\langle \Psi_{nm} \left| -\frac{e^2}{\epsilon r} \right| \Psi_{n'm'} \right\rangle = -\frac{2}{\epsilon} \int_0^\infty \int_0^{2\pi} \Psi_{nm} \frac{1}{r} \Psi_{n'm'}\, r\, dr\, d\phi \quad \ldots (18)$$

To perform the integral for radial part, we use of the Laguerre's polynomial relation[42]

$$\int_0^\infty y^{\mu-1} e^{-\kappa y} L_m^\tau(ay) L_n^\eta(by) dy = \frac{\Gamma(\mu)(\tau+1)_m(\eta+1)_n}{m!\, n!} \kappa^{-\mu} \sum_{j=1}^{m} \frac{(-m)_j(\mu)_j}{(\tau+1)_j j!} \left(\frac{a}{\kappa}\right)^j \sum_{\kappa=1}^{n} \frac{(-n)_j(\mu+j)_\kappa}{(\tau+1)_\kappa \kappa!} \left(\frac{b}{\kappa}\right)^\kappa \quad \ldots (19)$$

So, the impurity matrix term in Eq.19, is derived to be:

$$\left\langle \Psi_{nm} \left| -\frac{e^2}{\epsilon r} \right| \Psi_{n'm'} \right\rangle = \frac{2}{\epsilon} \frac{\Gamma\left(m+\frac{1}{2}\right)(m+1)_{n'}(m+1)_n}{n'!\, n!} \sum_{j=1}^{n} \frac{(-n)_j (m+\frac{1}{2})_j}{(m+1)_j j!} \sum_{\kappa=1}^{n'} \frac{(-n')_\kappa (m+j+\frac{1}{2})_\kappa}{(m+1)_\kappa \kappa!} \quad \ldots (20)$$

Now, to simplify the matrix element of the electric field term, reads as:

$$\langle \Psi_{nm} | eFr\, sin\theta cos\phi | \Psi_{,n'm'} \rangle = \sqrt{2}\, F\, sin\theta \int_0^\infty \int_0^{2\pi} \Psi_{nm}\, \Psi_{n'm'}\, r^2 dr\, cos\phi d\phi \quad \ldots (21)$$

In the last equation, the integration over ϕ isn't (2π), due to the presence of ($\cos\phi$), so to evaluate the integral, one can write $cos\phi$ to be equals $\frac{e^{-i\phi}+e^{+i\phi}}{2}$.

After using the relation in Eq. (19) we had two terms, $\frac{e^{-i\phi}}{2}$ and $\frac{e^{i\phi}}{2}$ multiplied by $\Psi_{n'm'}$, and these terms shifts m' to $m'-1$ (m' to $m'+1$), respectively, yielding selection rules as $\delta_{m',m'-1}(\delta_{m',m'+1})$. the complete expression of Eq. 21 can be given as,

$$\langle \Psi_{nm} | eFr\, sin\theta cos\phi | \Psi_{n'm'} \rangle = \frac{\sqrt{2}F\, sin\theta}{4} \left(\frac{\Gamma(m+1)(m+1)_{n'}(m+1)_n}{n'!\, n!} \sum_{j=1}^{n} \frac{(-n)_j (m+1)_j}{(m+1)_j j!} \sum_{\kappa=1}^{n'} \frac{(-n')_\kappa (m+j+1)_\kappa}{(m-1)_\kappa \kappa!} + \frac{\Gamma(m+2)(m+1)_{n'}(m+1)_n}{n'!\, n!} \sum_{j=1}^{n} \frac{(-n)_j (m+2)_j}{(m+1)_j j!} \sum_{\kappa=1}^{n'} \frac{(-n')_\kappa (m+j+2)_\kappa}{(m+2)_\kappa \kappa!} \right) \quad \ldots (22)$$

Now, after calculating all the energy matrix elements, our Hamiltonian matrix $H_{nn'}$ is ready, for diagonalization and obtaining the desired energy. These obtained QD energy spectra are used to investigate the dependence of (C_v) of QD on parameters (θ, B, F, T and ω_0) in addition to donor impurity. C_v is defined as the amount of heat required to change the temperature of that substance by one degree, and it can be computed using the temperature derivative of the statistical° energy[40]:

$$C_v = \frac{\partial \langle E(B,F,\theta,\omega_0,T \rangle}{\partial T} \quad \ldots (23)$$

3 Results and Discussion

In this work, all energy values are measured in units of effective Rydberg, as mentioned earlier. The computational work began with the first step which is to make sure that the computed energies by EDM are very accurate results. In our calculations, we changed the number of basis until convergent energy was achieved for various: ω_c,ω_0 and F listed in Tables (1-3). Furthermore, in Fig. 2 we have presented the number of basis effect on the ground state energy (E_G).Based on these convergency test, in our calculations, we have used a Hamiltonian matrix with dimensions: 72×72, where we have obtained

Table 1 — E_g vs. the basis of the matrix, at $\omega_0 = 3R^*, \omega_c = 2R^*, F = 5\ R^*$

No. of basis	E_g (meV)
0	-14.9319
18	-19.7069
30	-20.1743
42	-20.2128
54	-20.2154
66	-20.2155
78	-20.2155
90	-20.2155

Table 2 — E_g vs. the basis of the matrix at $\omega_0 = 3R^*, \omega_c = 3R^*, F = 5\ R^*$

No. of basis	E_g (meV)
0	-15.65
24	-20.2647
40	-20.7079
56	-20.7438
72	-20.7461
88	-20.7463
104	-20.7463
120	-20.7463

Table 3 — E_g vs. the basis of the matrix at $\omega_0 = 5R^*,\ \omega_c = 2R^*, F = 5\ R^*$

No. of basis	E_g(meV)
0	-16.9567
24	-24.1065
40	-25.6193
56	-25.9671
63	-26.0399
72	-26.0522
88	-26.076
104	-26.0831
120	-26.0852
136	-26.0854
152	-26.0858
168	-26.0859
184	-26.0859

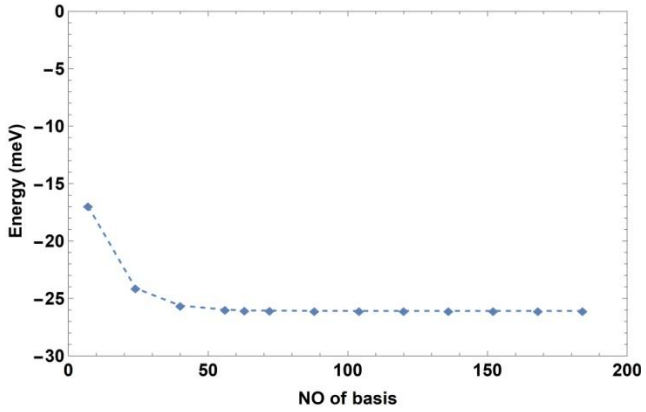

Fig. 2 — E_g *vs.* number of basis, for$\omega_0 = 2R^*, F = 5\ R^*$, $\omega_c = 2R^*, T = 1 \times 10^{-2}K$ and$\theta = 60^\circ$

numerical stable energy results listed in Table 3. Tables (1-3) and Fig. 2 show clearly the numerical stability of the energy matrix Hamiltonian. For example, E_G, in Table 1, is converged to $-20.2155\ meV$ although the number of basis increases from 66 to 90. After achieving the desired convergency, we calculate the binding energy($B.E$) of impurity in QD and present the results of $B.E$ of the donor impurity under several QD physical parameters. In Fig. 3, we have plotted $B.E$ against the magnetic field cyclotron frequency ω_c. The Figure

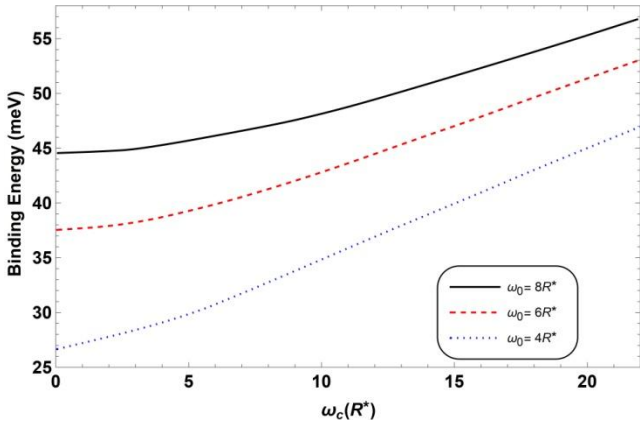

Fig. 3 — B.E *vs.*ω_c for, $F = 5\ R^*, T = 1 \times 10^{-2}K$ and $\theta = 60^\circ$

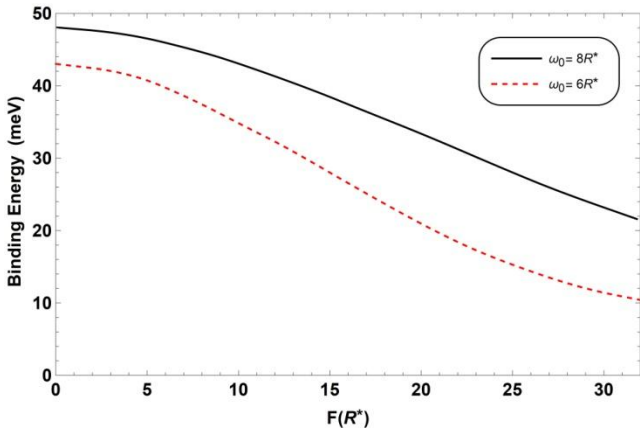

Fig. 4 — B.E *vs.* electric field for $\omega_c = 2\ R^*, T = 1 \times 10^{-2}K$ and$\theta = 60^\circ$

shows that $B.E$ increases as ω_c increases. This $B.E$ behavior is expected due to presence of a magnetic field which adds new parabolic confinement term for the electron as can be seen from Eq. 10 and that rises $B.E$. We have also shown the dependence of $B.E$, on the magnetic field for various confinements, $\omega_0 = 4R^*$, $6R^*$, and $8R^*$. The qualitative comparisons show that as the confinement frequency increases, the binding of the impurity enhances, as shown clearly in Fig. 3[37].

In addition, we have examined, in Fig. 4, the effect of electric field on the $B.E$ for different values of ω_0. As shown in the figure; $B.E$ decreases, as F increases, since the field appears to detach the electron from the nucleus and drive it further, which leads to less Coulomb interaction energy, and in this case,$B.E$decreases. The numerical$B.E$ results are also presented in Table 4.

Figure 5 shows the change in $B.E$ due to the change of the tilted angle of the electric field θ. In that figure, as θ increases, the component of electric

Table 4 — B. E for different values of electric field (F) and ω_0, at $\omega_c = 2R^*, T = .01K, \theta = 60°$

F(R*)	B.E (meV) (ω_0 = 6R*)	B.E (meV) (ω_0 =8R*)
0	43.058	47.814
4	41.522	46.991
8	37.554	44.716
12	32.257	41.416
16	26.462	37.513
20	20.848	33.327
24	16.085	29.1
28	12.599	25.035
32	10.286	21.314

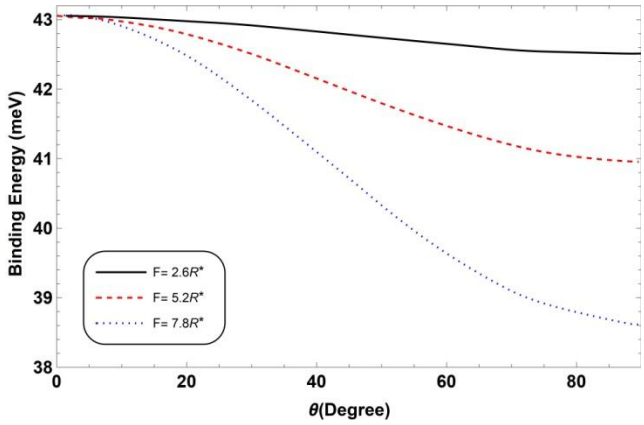

Fig. 5 — B.E *vs.* θ for $\omega_0 = 2R^*, \omega_c = 2R^*$ and $T = 1 \times 10^{-2}K$

field increases, having the same effect on $B.E$ as Fincreases, and the figure also shows the dependence of $B.E$ on the electric field.

All the results shown in the figures mentioned above are in good qualitative agreement with the reported results in[37,43].

as an essential quantity to achieve the desired results for the QD's thermal properties, we calculated the statistical energy $< E >$, from which one can find$C_v$as defined in Eq. (23). The electric field effect on $< E >$is plotted in Fig. 6. The figure shows that, for fixed ω_c-values, as the electric field strength gets higher, $< E >$ decreases due to larger separation distance between electron and impurity.

In Fig. 7, for fixed values of temperature, as B increases, so does $< E >$, which is a result of the extra confinement by the magnetic field, and by changing the temperature, the figure shows that for higher temperatures, $< E >$ is greater as the electron gains more thermal energy, and this behavior is consistent with the results reported in[41].The effect of ω_0 on $< E >$of the donor impurity is presented in Fig. 8, where we can see that, for fixed values of $\omega_c, < E >$ enhances significantly as the $\omega_0$increases.

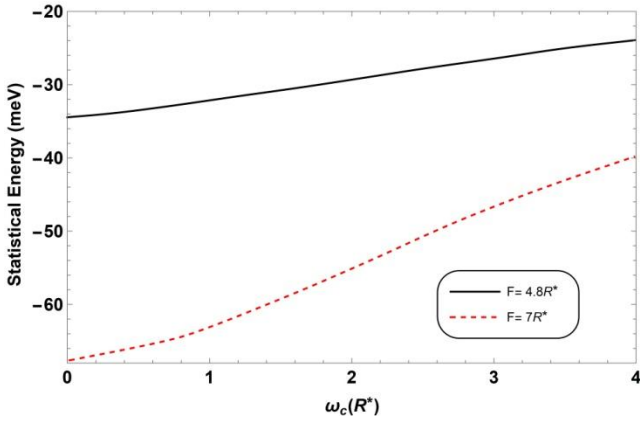

Fig. 6 — ⟨E⟩ against ω_c for, $\omega_0 = 2R^*, \theta = 60^0$ and $T = 1 \times 10^{-2}K$

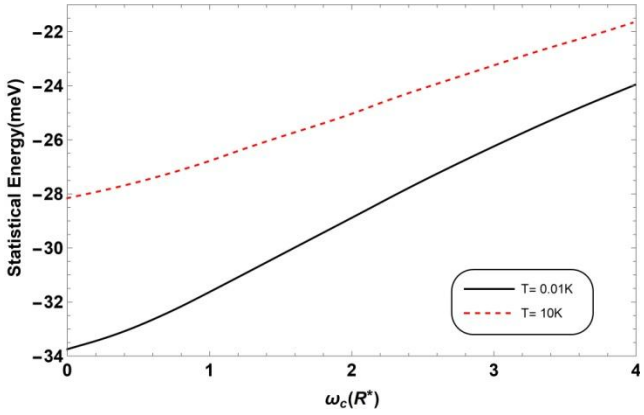

Fig. 7 — ⟨E⟩ against ω_c for $\omega_0 = 2R^*, F = 5\,R^*$ and $\theta = 60^\circ$

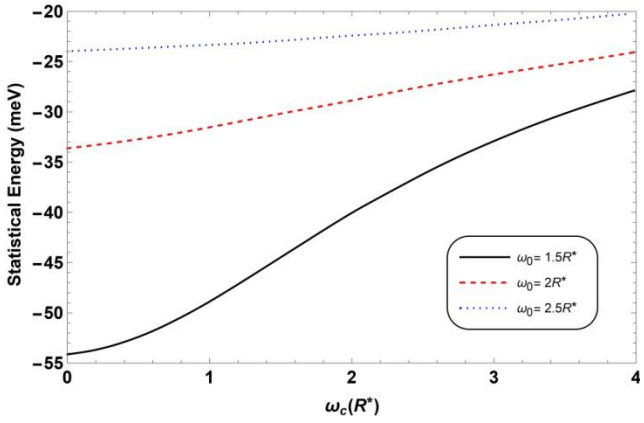

Fig. 8 — ⟨E⟩ against ω_c for, $F = 5\,R^*$, $\theta = 60^\circ$ and $T = 1 \times 10^{-2}K$

This result is in qualitative agreement with[41] In addition, Fig. 9 shows the changing of the tilt angle θ affects $< E >$, since as θ increases, the electric field term increases. In this case, B.E of the impurity decreases since the Coulomb energy reduces, $(\sim 1/r)$ also, as we explained earlier in the discussion. The

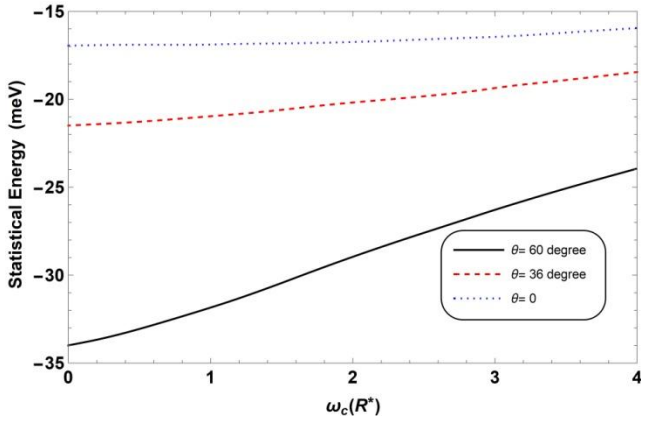

Fig. 9 — ⟨E⟩ against ω_c for $\omega_0 = 2R^*$, $F = 5\,R^*$ and $T = 1\times10^{-2}K$

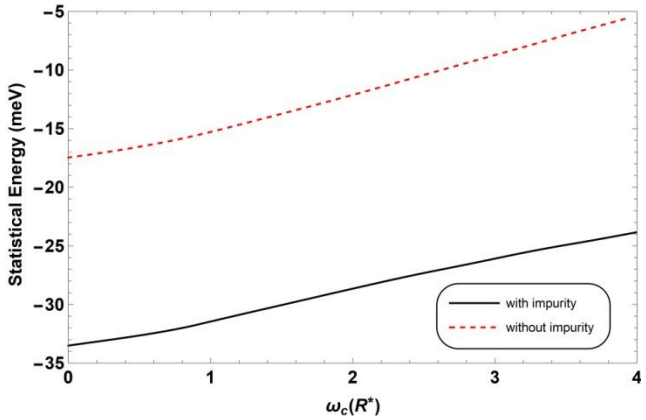

Fig. 10 — ⟨E⟩ against ω_c for $\omega_0 = 2R^*$, $F = 5R^*$, $\theta = 60^\circ$ and $T = 1\times10^{-2}K$

presence of impurity on $< E >$of the electron is very important and is found to reduce $< E >$as shown in Fig. 10 due to the negative coulomb energy contribution. This in turn affects the thermal properties of the QD.

Furthermore, we have investigated C_v of the electron confined in a QD taking into account various physical QD parameters. The variation of C_v as a function of temperature for different strength of electric field are shown in Fig. 11. The figure shows that the as the temperature increases C_v reaches a 2D limit, $C_v = 2k_B$. This limit behavior for C_v is also in agreement with[37,43-44]. In this case, for high values of F, C_v is large, but at certain T (about $90\,K$) there is intersection and a flip in the C_v-behavior, so at high $T(T > 90\,K)$, C_v is smaller for high electric fields. As F increases, $B.E$ of the donor impurity decreases, and in this case, C_v decreases as shown in Fig. 11. The effect of the presence of impurity on the C_v is illustrated in Fig. 12 where, we can notice that for low temperature values ($T < 90\,K$), C_v is larger without

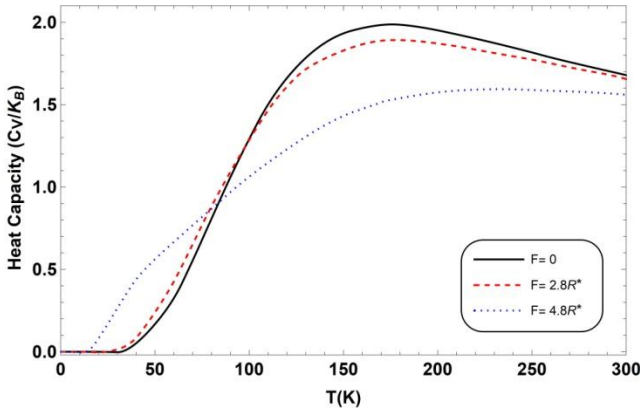

Fig. 11 — C_v against T for $\omega_0 = 2R^*$, $\omega_c = 2R^*$ and $\theta = 60^\circ$

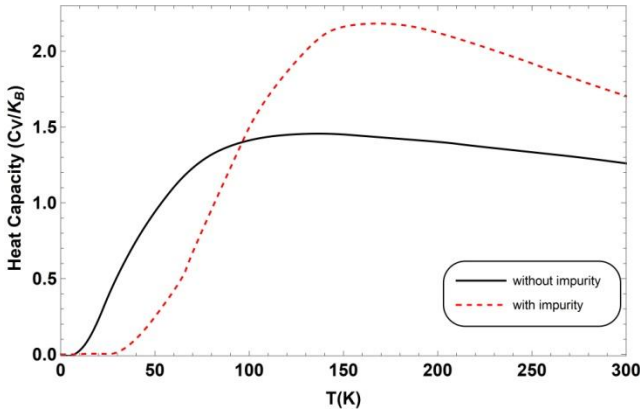

Fig. 12 — C_v against T for $\omega_0 = 2R^*$, $\omega_c = 2R^*$ and $\theta = 60^\circ$

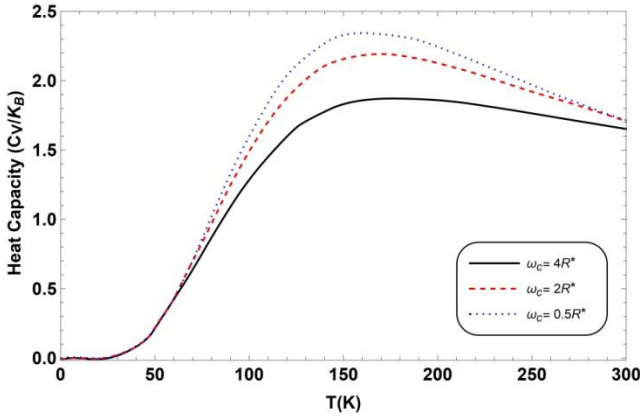

Fig. 13 — C_v against T for $F = 1.8\,R^*$, $\omega_0 = 2R^*$ and $\theta = 60^\circ$

impurity, but when the temperature gets higher, the situation is reversed, and C_v is larger when there is an impurity.

Finally, the magnetic field effect on C_v is presented in Fig. 13, where it shows that the effect of the magnetic field appears at high temperature ($T > 70\,K$) where C_v is larger as the magnetic field is smaller.

4 Conclusion

Using diagonalization method, The Hamiltonian of donor impurity in quantum dot had solved in presence of magnetic and tilted electric fields, as well as a parabolic confinement potential. We have investigated the dependence of $B.E$ onelectric field parameters (strength, tilt angle), and confinement strength. The results are in good agreement with previously published studies [37,41,43-44]. Moreover, $B.E$ and $\langle E \rangle$ were investigated as a function of system tunable parameters (ω_c , ω_0, F,T). It was found that rising either F or θ decreases $\langle E \rangle$.The temperature has also an important effect on $\langle E \rangle$.

As a final step, the effect of electric field on (C_v) was discussed. The current study shows that, at low temperature, C_v is higher for higher F, while for higher temperatures, the situation is reversed.

References

1 Harrison P, *John Wiley & Sons, Chichester*, 2005.
2 Tiwari S, Rana F, Chan K, Shi L & Hanafi H, *Appl Phys Lett*, 69 (1996) 1232.
3 Schwarz J A, Contescu C I & Putyera K, *CRC press*, 3 (2004).
4 Bahramiyan H & Khordad R, *Opt Quant Electron*, 46 (2014) 719.
5 Xu Y B, Hassan S S A, Wong P K J, Wu Jian, Claydon J S, Lu Y X, Damsgaard C D, Hansen J B, Jacobsen C S & Zhai Y, *IEEE Trans Magnet*, 44 (2008) 2959.
6 Li S S & Xia J B, *J Appl Phys*, 101 (2007) 093716.
7 Bose C & Sarkar C K, *Phys B: Condensed Matter*, 253 (1998) 238.
8 Kırak M, Yılmaz S, Sahin M & Gencaslan M, *J Appl Phys*, 109 (2011) 094309.
9 Murillo G & Porras-Montenegro N, *Physica Status Solidi(b)*, 220 (2000) 187.
10 Bose C, *J Appl Phys*, 83 (1998) 3089.
11 Zhu J L, Xiong J J & Gu B L, *Phys Rev B*, 41 (1990) 6001.
12 Li S S & Xia J B, *J Appl Phys*, 101 (2007) 093716.
13 Porras-Montenegro N & Pe S T, *Phys Rev B*, 46 (1992) 9780.
14 Charrour R, Bouhassoune M, Fliyou M & Nougaoui A, *Phys B: Condensed Matter*, 293 (2000) 137.
15 Sali A, Kharbach J, Rezzouk A & Jamil M O, *Super Latt Microstruct*, 104 (2017) 93.
16 Baser P & Elagoz S, *Superlatt Microstruct*, 102 (2017) 173.
17 Turkyilmazoglu M, *The Europ Phys J Plus*, 135 (2020) 781.
18 Turkyilmazoglu M, *Comput Meth Prog Biomed*, 87 (2020) 105171.
19 Ciftja O, *J Phys: Condensed Matter*, 19 (2007) 046220.
20 Tanaka K, *Annals Phys*, 268 (1998) 31.
21 Soylu A, *Annals Phys*, 327 (2012) 3048.
22 Karimi M J & Rezaei G, *Phys B: Condensed Matter*, 406 (2011) 4423.
23 Wang D, Jin G, Zhang Y & Ma Y Q, *J Appl Phys*, 105 (2009) 063716.
24 Liang S J & Xie W F, *The Europ Phys J B*, 81 (2011) 79.
25 Akbas H, Erdogan I & Akankan O, *Superlatt Microstruct*, 50 (2011) 80.
26 Ghosh A & Ghosh M, *Superlatt Microstruct*, 104 (2017) 438.
27 Eshghi M, Mehraban H & Ikhdair S M, *arXiv preprint archiv*, (2017) 1704.00776.
28 Faten B, Ayham Shaer & Elsaid M K, *J Taibah Univ Sci*, 11.6 (2017) 1122.
29 Boda A & Chatterjee A, *Superlatt Microstruct*, 97 (2016) 268.
30 Tojo T, Inui M, Ooi R, Takeda K & Tokura Y**,** *Jpn J Appl Phys*, 56 (2017) 075201.
31 Boda A, Boyacioglu B, Erkaslan U & Chatterjee A, *Phys B: Condensed Matter*, 498 (2016) 43.
32 Pournaghavi N, Esmaeilzadeh M, Abrishamifar A & Somaieh A M, *J Phys: Condensed Matter*, 29 (2017) 145501.
33 Sinova J, Culcer D, Niu Q, Sinitsyn N A, Jungwirth T & Mac-Donald A H, *Phys Rev Lett*, 92 (2004) 126603.
34 Hwang T M, Lin W W, Wang W C & Wang W, *J Comput Phys*, 196 (2004) 208.
35 Johnson H T, Freund L B, Akyuz C D & Zaslavsky A, *J Appl Phys*, 84 (1998) 3714.
36 El-Said M, *Phys B: Condensed Matter*, 202 (1994) 202.
37 Rezaei G & Kish S S, *Phys E: Low-Dimens Syst Nanostruct*, 45 (2012) 56.
38 El-Said M, Ali M & Shaer A, *Bagh Sci J*, 18(2), 0409-0409.
39 Alia A, Elsaid M & Shaer A, *J Taibah Univ Sci*, 13 (2019) 687.
40 Boyacioglu B & Chatterjee A, *J Appl Phys*, 112 (2012) 083514.
41 Nammas F S, *Phys A: Statist Mech Appl*, 508 (2018) 187.
42 Shaer Ayham, El-Said Mohammad & Elhasan Musa, *Turk J Phys*, 40 (2016) 209.
43 Castano-Yepos J D, Amor-Quiroz D A, Ramirez-Gutierrez C F & Gomez E A, *Phys E*,109 (2019) 59.
44 Gumber S, Kumar M, Jha P K & Mohan M, *Chin Phys B*, 25 (2016) 056502.